

Contribution of intrinsic and synaptic factors in the desynchronization of thalamic oscillatory activity

I. Timofeev^{a,*}, M. Bazhenov^b, T.J. Sejnowski^{b,c}, M. Steriade^a

^a *Laboratory of Neurophysiology, School of Medicine, Laval University, Québec, Canada G1K 7P4*

^b *Computational Neurobiology Laboratory, Howard Hughes Medical Institute, The Salk Institute, 10010 North Torrey Pines Road, La Jolla, CA 92037, USA*

^c *Department of Biology, University of California, La Jolla, CA 92093, USA*

Abstract

The interplay between the intrinsic properties of thalamocortical (TC) neurons and synaptic potentials was investigated in vivo, in decorticated and intact-cortex cats, as well as in computational models to elucidate the possible mechanisms underlying the disruption of the spindle oscillation, a network phenomenon. We found that the low-threshold spikes (LTSs) in TC neurons were graded in their amplitude and latency to peak when elicited by current pulses or synaptic potentials from physiological levels of hyperpolarization. IPSPs could either delay or shunt the LTSs. Although the onset of spindles was rhythmic and did not include rebound LTSs, the end of spindles was highly aperiodic suggesting that desynchronization could contribute to the spindle termination. The desynchronization could have several sources, the main of which are (a) intrinsically generated rebound LTSs in TC neurons that occur with different delays and keep thalamic reticular (RE) neurons relatively depolarized, and/or (b) out-of-phase firing of cortical neurons due to intracortical processes that would result in depolarization of both TC and RE neurons. The present study suggests that an active cortical network participates in disrupting the spindle activities. We propose that the progression of spindles contains at least three different phases, with different origins: (a) the onset is generated by RE neurons that impose their activity onto TC neurons, without participation of cortical neurons; (b) the middle part is produced by the interplay between RE and TC neurons, with potentiation from the cortical network; and (c) the waning of spindles is due to the out-of-phase firing of TC and particularly cortical neurons that participate in the spindle termination. © 2001 Elsevier Science Ltd. All rights reserved.

Keywords: Intrinsic; Synaptic; Low-threshold spike; Spindles; Desynchronization

1. Introduction

States of vigilance are characterized by various forms of oscillatory activity in the thalamocortical network, whose mechanisms and sources of generation are different (Steriade et al., 1993a). (a) The slow sleep oscillation (<1 Hz) arises within the neocortex since it survives ipsilateral thalamectomy (Steriade et al., 1993b) and is absent in the thalamus of decorticated animals (Timofeev and Steriade, 1996). Recent in vivo recordings and modeling studies suggest that a large number of interconnected neocortical neurons is essential to generate the cortical slow oscillation (Timofeev et al., 2000). (b) The clock-like delta activity (1–4 Hz) has an intrathalamic origin and is due to the interaction of two of the intrinsic currents (I_h and I_T) in thalamocortical (TC) neurons (McCormick and Pape, 1990; Leresche et al., 1991; Soltesz et al., 1991; Curró Dossi et al., 1992). Synchrony between different TC neurons during delta activ-

ity has not been found in decorticated cats (Timofeev and Steriade, 1996). However, the presence of a corticothalamic feedback in intact-brain animals could synchronize thalamic burst-firing at delta frequency and generate strong field potentials (Steriade et al., 1991; Curró Dossi et al., 1992). At a certain level of leak current (I_{leak}), the ‘window’ component of I_T may create oscillations similar in frequency to the intrinsic thalamic delta oscillation (Williams et al., 1997). Another component of delta activity is cortical in origin, as delta waves can be recorded from neocortex after thalamectomy (Villablanca et al., 1974; Ball et al., 1977; Steriade et al., 1993b), but its cellular mechanisms remain to be elucidated. (c) Spindle activity (7–15 Hz) is generated within intrathalamic networks (reviewed in Steriade et al. (1997)). Spindles are initiated in the reticular thalamic (RE) nucleus, where they occur even after disconnection from the remaining thalamus (Steriade et al., 1987; Bazhenov et al., 1999, 2000b; Houweling et al., 2000). They are fully synchronized by RE–TC interconnections (Steriade et al., 1993a; von Krosigk et al., 1993) and especially by corticothalamic inputs (Contreras et al., 1996, 1997). In vitro studies

* Corresponding author. Tel.: +1-418-656-5166; fax: +1-418-656-7898. E-mail address: igor.timofeev@phs.ulaval.ca (I. Timofeev).

have shown that spindles are terminated by Ca^{2+} -induced up-regulation of I_h (Bal and McCormick, 1996; Lüthi and McCormick, 1998a,b). Spike-bursts crowning low-threshold spikes (LTSs) in TC neurons are not generated during the initial cycles of spindles (Bazhenov et al., 2000b), suggesting a passive involvement of TC neurons in at least this early phase. The spindle termination may be mediated not only via I_h , but also by slightly different duration of the IPSPs leading to desynchronization of activity, as originally suggested by Andersen and Andersson (1968). Indeed, a moderate modulation of LTSs has a profound desynchronizing effect on paroxysmal oscillations (Huguenard and Prince, 1994). This indicates that both intrinsic currents and synaptic events may be responsible for the disruption of some forms of rhythmic activity generated within the thalamus.

We show here that the interaction of some intrinsic currents and synaptic potentials may lead to the termination of oscillations generated in thalamic networks. We emphasize (a) the graded nature of LTSs in TC neurons; (b) the interaction between LTSs and postsynaptic potentials (PSPs); and (c) the mechanisms through which LTS–PSP coupling produces a desynchronization of network activity, leading to spindle termination.

2. Methods

2.1. *In vivo* experiments

Experiments were carried out on 48 adult cats with unilateral decortication, anesthetized either with ketamine–xylazine (10–15 and 2–3 mg/kg, i.m.; $n = 42$) or urethane (1.8 g/kg, i.p.; $n = 6$), and on 62 cats with intact cortex anesthetized with ketamine–xylazine ($n = 25$) or with sodium pentobarbital (35 mg/kg, i.p.; $n = 37$). The electroencephalogram (EEG) was monitored continuously during the experiments to ascertain the depth of the anesthesia. Additional doses were given at the slightest tendency toward an activated EEG pattern. The tissue to be excited and the pressure points were infiltrated with lidocaine (2%). The cats were paralyzed with gallamine triethiodide only after the EEG showed typical signs of deep anesthesia and were ventilated artificially with the control end-tidal CO_2 at 3.5–3.8%. The rectal temperature was monitored and maintained at 37–38°C and the heart rate was 90–110 beats/min. Saline glucose was given every 6 h as a fluid therapy during the experiments that lasted for ~12 h. In some experiments the left cortex was ablated by suction and the corpus callosum was cut (see histology in Timofeev and Steriade (1996) and Steriade and Timofeev (1997)). The stability of intracellular recordings was ensured by bilateral pneumothorax, cisternal drainage, hip suspension, and by filling the holes that were opened in the skull with a warm agar solution (4% in 0.9% saline). At the end of experiments, the animals were given a lethal dose of pentobarbitone and perfused intracardially with physiological saline, followed by 10%

formaldehyde. The extent of hemidecortication, the callosal cuts and the position of stimulating electrodes were verified on coronal sections (80 μm) stained with thionine. The experimental protocol has been approved by the committee for animal care in our university and also conforms to guidelines recommended by the National Institute of Health.

Intracellular recordings in current-clamp mode were performed with glass micropipettes filled with a solution of 3 M potassium acetate and having dc resistance of 30–80 M Ω . Recordings were made from the left ventrolateral (VL), lateral posterior (LP) or RE thalamic nuclei and from cortical areas 4, 5 and 7. Simultaneous dual intracellular recordings were made from two VL neurons, or VL and RE neurons, in decorticated cats, and from VL and area 4 neurons in intact-cortex animals. A high impedance amplifier with active bridge circuitry was used to record potential and inject current into cells. Field potentials were recorded by means of bipolar coaxial electrodes. Surface and depth or bipolar (between surface and depth) EEG was recorded from the right cortex in experiments on decorticated animals and usually from the vicinity of intracellular pipettes in intact-cortex cats. Thalamic field potentials were obtained from the VL nucleus in monopolar mode. The signals were recorded on an eight-channel tape with a band pass 0–9 kHz, digitalized at 20 kHz for off-line computer analysis. The amplitude of LTS was measured from the baseline membrane potential to the maximal depolarization reached by TC neuron during LTS excluding fast spikes.

2.2. Model

We simulated two network models: (1) a one-dimensional two-layer chain of 15×2 RE–TC cells and (2) a one-dimensional four-layer chain of 21×4 thalamic (RE–TC) and cortical pyramidal (PY) and interneuron (IN) cells. The diameters of the connection fan out for RE \leftrightarrow RE (GABA_a), RE \rightarrow TC (GABA_a + GABA_b) and TC \rightarrow RE (AMPA) connections in the first model were 3 cells. In the second model the diameters of the connection fan out were 5 cells for RE \leftrightarrow RE (GABA_a), RE \rightarrow TC (GABA_a + GABA_b), TC \rightarrow RE (AMPA), PY \leftrightarrow PY (AMPA + NMDA), PY \rightarrow IN (AMPA + NMDA), IN \rightarrow PY (GABA_a) connections and 10 cells for TC \rightarrow PY (AMPA), TC \rightarrow IN (AMPA), PY \rightarrow TC (AMPA), PY \rightarrow RE (AMPA) connections. The maximal conductance for each synapse was scaled to keep the total maximal conductance from all synapses onto a cell fixed. A simple model was used to describe short-term depression of excitatory and inhibitory synaptic connections between cortical neurons (Tsodyks and Markram, 1997; Galarreta and Hestrin, 1998).

Each TC and RE cell was modeled by a single compartment that included voltage- and Ca^{2+} -dependent currents described by Hodgkin–Huxley kinetics. The set of the intrinsic currents used to model a TC cell included fast Na^+ current ($g_{\text{max}} = 90 \text{ mS/cm}^2$), fast K^+ current ($g_{\text{max}} = 10 \text{ mS/cm}^2$), I_T ($g_{\text{max}} = 1.5\text{--}2 \text{ mS/cm}^2$), I_h ($g_{\text{max}} =$

0.005–0.02 mS/cm²) and I_{leak} . To model an RE cell, we included fast Na⁺ current ($g_{\text{max}} = 100$ mS/cm²), fast K⁺ current ($g_{\text{max}} = 10$ mS/cm²), I_T ($g_{\text{max}} = 2.1$ mS/cm²) and I_{leak} . The cortical neurons were modeled by two compartmental models (10 M Ω resistance between compartments) as in a previous paper (Mainen and Sejnowski, 1996), with the addition of persistent Na⁺ current I_{NaP} (Alzheimer et al., 1993; Kay et al., 1998; Timofeev et al., 2000) ($g_{\text{max}} = 0.07$ mS/cm²). The firing properties of this model depend on the coupling conductance between compartments and the ratio of axo-somatic area to dendritic area r (Mainen and Sejnowski, 1996). We used a model of a regular-spiking neuron for PY cells ($r = 165$) and a model of a fast-spiking neuron for IN cells ($r = 50$).

GABA_a, AMPA and NMDA synaptic currents were modeled by first-order activation schemes. GABA_b receptors were modeled by a higher-order reaction scheme that took into account activation of K⁺ channels by G-proteins (Destexhe et al., 1996). The maximal conductances were $g_{\text{AMPA}} = 0.15$ μ S between PY cells, $g_{\text{NMDA}} = 0.01$ μ S between PY cells, $g_{\text{AMPA}} = 0.05$ μ S from PY \rightarrow IN, $g_{\text{NMDA}} = 0.008$ μ S from PY \rightarrow IN, $g_{\text{AMPA}} = 0.025$ μ S from PY \rightarrow TC, $g_{\text{AMPA}} = 0.05$ μ S from PY \rightarrow RE, $g_{\text{GABA}_a} = 0.05$ μ S from IN \rightarrow PY, $g_{\text{AMPA}} = 0.05$ μ S from TC \rightarrow PY, $g_{\text{AMPA}} = 0.05$ μ S from TC \rightarrow IN, $g_{\text{GABA}_a} = 0.2$ μ S between RE cells, $g_{\text{GABA}_a} = 0.2$ μ S from RE \rightarrow TC, $g_{\text{GABA}_b} = 0.04$ μ S from RE \rightarrow TC and $g_{\text{AMPA}} = 0.4$ μ S from TC \rightarrow RE.

The expressions for voltage- and Ca²⁺-dependent transition rates for all intrinsic currents and the rate constants for all synaptic kinetic equations are given in Bazhenov et al. (1998a,b) and Timofeev et al. (2000).

3. Results

3.1. Database and neuronal properties

Intracellular recordings were made from >500 TC neurons in thalamic VL and LP nuclei and >1000 cortical cells in areas 4, 5 and 7. The electrophysiological identification of a TC neuron is shown in Fig. 1 (left column). Small depolarization of this TC neuron with intracellular dc current produced passive responses. Increases in the intensity of the depolarizing current resulted in a progressively increased number of action potentials and a persistent depolarization (Fig. 1, top trace in left column) that is probably generated by I_{NaP} (Jahnsen and Llinás, 1984b; Parri and Crunelli, 1998). At the offset of the depolarizing current pulse most TC neurons generated a slow afterhyperpolarizing potential (Fig. 1, top trace in left column). Application of low-amplitude hyperpolarizing current pulses resulted in passive responses. An increase in the pulse amplitude hyperpolarized the TC neuron to a level of activation of I_h that produced a depolarizing sag. At the offset of the hyperpolarizing current pulse, the TC neuron generated a depolarizing

response, commonly called LTS for low-threshold spike, that is due to the de-inactivation of I_T (Jahnsen and Llinás, 1984a,b; Hernández-Cruz and Pape, 1989; Tarasenko et al., 1997). Recent studies suggest that the LTS also contains a component mediated by I_{NaP} (Parri and Crunelli, 1998). An increase in the amplitude of the hyperpolarizing current pulse produced an increase in both the depolarizing sag and the rebound excitation that led to a burst of up to eight Na⁺ spikes. An even stronger hyperpolarization activated the I_h that was able to trigger an LTS before the end of the current pulse (Fig. 1, bottom trace in the left column). Thus, the increase in the amplitude of the hyperpolarizing current pulse from a common membrane potential (−67 mV) resulted in LTSs that were different in amplitude, latency and number of fast Na⁺ spikes crowning the LTSs. The interaction of LTS with IPSPs (Fig. 1, right column) yield to specific phenomena that are described later.

Neocortical neurons were electrophysiologically identified as regular-spiking (RS), fast-spiking (FS), intrinsically-bursting (IB) and fast-rhythmic bursting (FRB) according to their responses to intracellularly applied depolarizing current pulses (Connors and Gutnick, 1990; Nuñez et al., 1993; Gray and McCormick, 1996; Steriade et al., 1998). Out of these four cellular types, only the FS neurons displayed linear current–frequency relations. The RS neurons revealed significant spike frequency adaptation and in FRB cells the number of spikes increased as a function of the injected current within certain level of depolarization, but maintained spike-burst repetition at frequencies around 30–40 Hz. The IB neurons generated bursts at frequencies around 7 Hz that might be followed by a tonic firing tail. Thus, the intrinsic responses of neocortical neurons modify input signals and their output does not linearly depend on activities in input structures, with the exception of FS neurons.

3.2. Graded nature of LTS in TC neurons

The variability of LTSs generated by the same neuron in responses to hyperpolarizing current pulses was investigated in detail in 28 neurons. A typical example is depicted in Fig. 2. The baseline membrane potential of this neuron was −70 mV. At the brake of the hyperpolarizing current pulse (0.1 s duration, 1.6 nA) the neuron rebounded with a stereotyped LTS that was crowned by four fast Na⁺ spikes (top left). Decreasing the amplitude of the hyperpolarizing current pulse to 1 nA resulted in a smaller number of spikes, but the response remained stereotyped for a given intensity of hyperpolarization. When threshold hyperpolarizing current pulses (−0.8 nA) were used, the LTS response became extremely variable (Fig. 2A, right). The level of membrane potential during these hyperpolarizing current pulses (−0.8 nA) reached −78 mV. This value often occurs in TC neurons during spindles (see Fig. 7), suggesting an intrinsic variability in LTS generation during spindles. Slight, spontaneously occurring changes in input resistance were effective in either preventing the LTS or eliciting LTSs of different

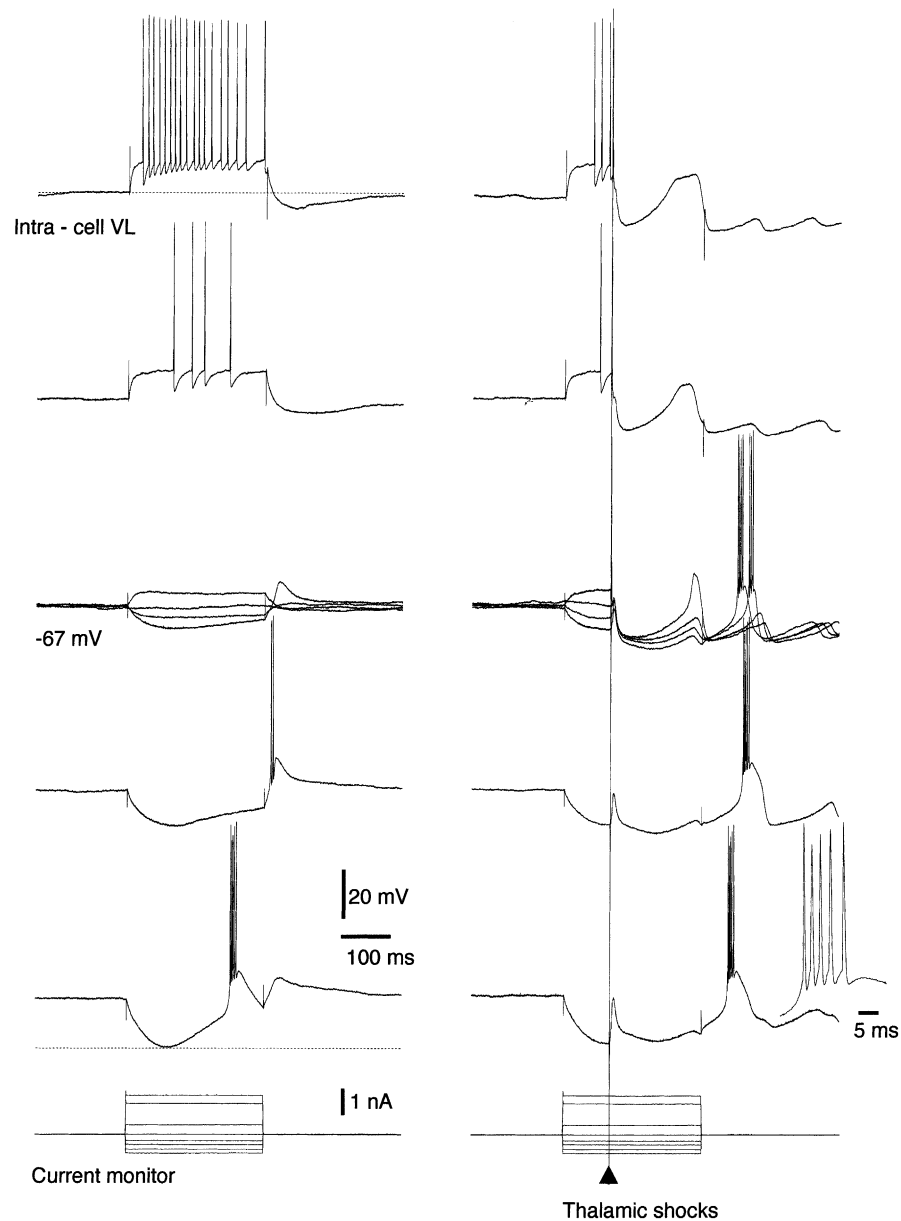


Fig. 1. Intrinsic electrophysiological properties and their interaction with synaptic responses in thalamocortical neurons (barbiturate anesthesia). Left column shows responses of thalamocortical neuron from VL nucleus to intracellularly applied current pulses during periods free of large synaptic events. In the right column, local thalamic stimuli, marked by triangle, were applied during the current pulses. Note the delays in generation of rebound LTS' in right column.

amplitude and latencies, with or without Na^+ spikes. The variations of LTS amplitudes and times to a maximal depolarization from the experiment shown in the upper panels of Fig. 2 are depicted below in plots indicating that the TC neuron could generate rebound LTS in a range of 1–15 mV (Fig. 2B) and with latency to peak from 20 to almost 100 ms (Fig. 2C). Note that, following an increase in hyperpolarization, the LTS first reaches its maximal amplitude and then a decrease of latency (Fig. 2D). Thus, full LTS could occur with significant delays.

The graded properties of the LTS were analyzed in models of an isolated TC cell or isolated RE–TC pair (Fig. 3). A

hyperpolarizing dc pulse (0.1 s duration) was applied to activate the low-threshold Ca^{2+} current leading to an LTS. The LTS amplitude was sensitive to the TC-cell's membrane potential during the imposed hyperpolarization: changing the resting potential by ± 2 mV was sufficient to transform an LTS in isolation to an LTS followed by a single action potential or a doublet (Fig. 3A). An essential feature was the timing of the rebound excitation, which strongly depended on the intrinsic properties of the TC cell. An increase or decrease of the I_T conductance, accompanied by a corresponding change of the I_h to keep the membrane potential at the same level, led to significant variations of the LTS time delay

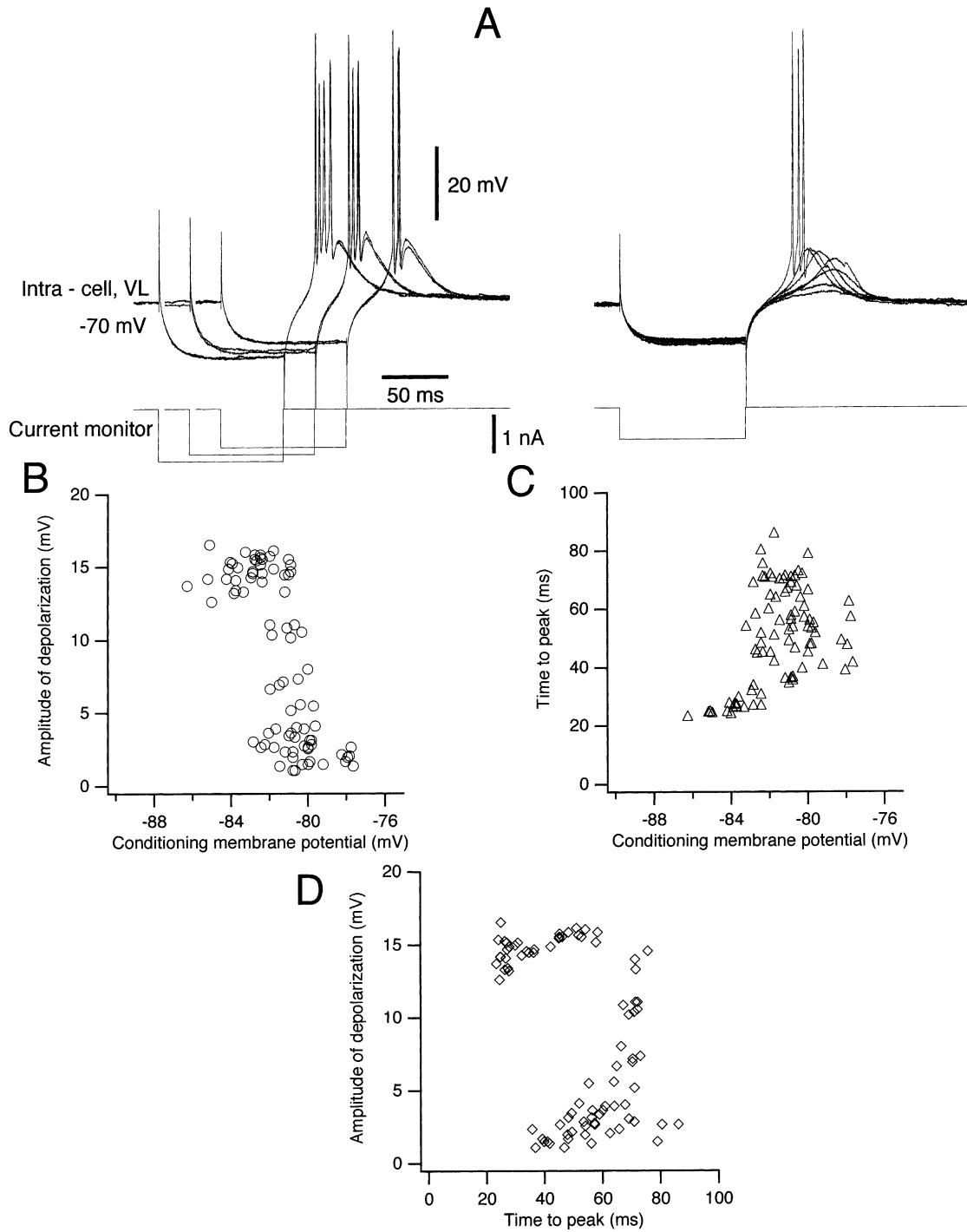


Fig. 2. LTSs in thalamocortical neurons are graded in amplitude and latency of peak (ketamine–xylazine anesthesia; decorticated hemisphere). Panel A shows low-threshold responses generated at a termination of 100 ms hyperpolarizing current pulses. Note stability and graded nature of responses as a function of applied current pulse (left) and great fluctuations in time and amplitude at threshold hyperpolarization (right). Plots below indicate graded responses in voltage (B) and time-to-peak (C). Conditioning membrane potential is the membrane potential just before the end of the current pulse. Amplitude of maximal depolarization is calculated from baseline membrane potential. Time-to-peak is the time from the end of current pulse to the maximal depolarization excluding fast spikes. (D) LTS reaches its maximal amplitude first and then the latency to peak decreases.

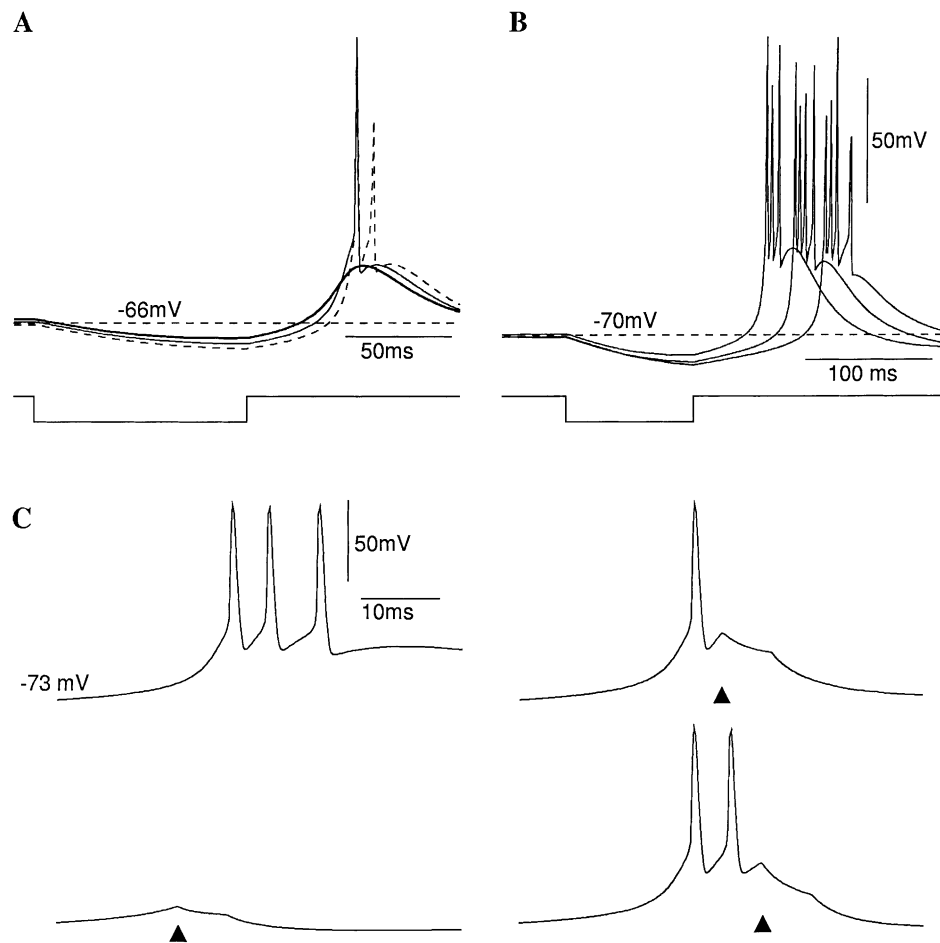


Fig. 3. Properties of LTSs in modeled neurons. Negative dc current (100 ms duration) was applied to an isolated TC cell (A and B) or to the TC cell from an isolated RE–TC pair (C). (A) Small variations of the resting membrane potentials (± 2 mV) elicited an LTS in isolation, LTS accompanied with single spike or with a burst of two action potentials (B). Variations of the maximal conductances for I_T (between 1.5 and 2 mS/cm²) and I_h (between 0.005 and 0.02 mS/cm²) significantly altered LTS delay time. (C) Shunting effect of RE-evoked IPSP on LTS in TC neurons. Upper left panel shows intact LTS in TC neuron. Spike in RE cell (marked by triangle) evoked IPSP leading to earlier LTS termination.

— about 60 ms in these simulations (Fig. 3B). This variable delay was an important factor for spindle termination.

In previous investigations, the removal of the cortex resulted in the hyperpolarization of TC neurons (Curró Dossi et al., 1992; Timofeev and Steriade, 1996). At these hyperpolarized levels, some spontaneous synaptic events were able to trigger LTSs. Fig. 4 depicts a period of spontaneous activity of a TC neuron from the VL nucleus of decorticated thalamus that received spontaneous EPSPs of presumably cerebellar origin (see Timofeev and Steriade, 1997). Due to slow spontaneous fluctuations of the membrane potential, the spontaneous EPSPs reached the TC neuron at different voltages. When the neuron was polarized below -75 mV, those low amplitude EPSPs did not elicit regenerative responses because low amplitude EPSPs were not able to depolarize the neuron sufficiently to reach the threshold for LTS generation (Fig. 4). However, when the neuron had a membrane potential between -75 and -65 mV, such spontaneous EPSPs sometime elicited LTSs that varied significantly in their amplitudes as well as their latencies to peak. Similar

results were obtained by application of small depolarizing current pulses in spontaneously hyperpolarized TC neurons of the decorticated hemisphere (not shown).

A few hours after decortication, 60% of TC neurons produced spontaneously an intrinsically generated delta activity that was not synchronized with other TC neurons (see Fig. 14 in Timofeev and Steriade, 1996). The LTSs produced during this activity had different amplitudes that did not, however, affect the frequency of the intrinsic delta oscillation (Fig. 5). Periods of spontaneously occurring waxing and waning delta activity were rare ($n = 5$ out of 257 neurons recorded in decorticated cats). Nonetheless, the application of long-lasting hyperpolarizing current pulses produced a continuous clock-like delta oscillations in most (85%) of the TC neurons, with LTSs of different amplitudes that were a function of the injected hyperpolarizing current (Fig. 6). We emphasize that the frequency of delta activity, occurring spontaneously or elicited by hyperpolarizing pulses was stable, or only slightly changing, for most of the neurons (57 out of 65 tested), despite the fact that the amplitudes of

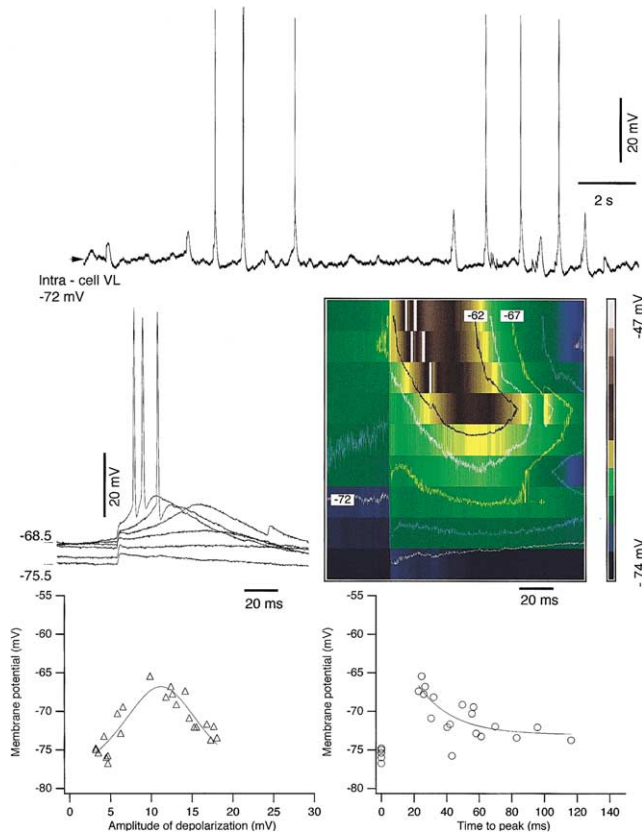


Fig. 4. Spontaneous EPSPs elicit gradual LTSs. Unilateral decortication (ketamine–xylazine anesthesia). Following decortication the membrane potential of TC neuron from VL nucleus is relatively hyperpolarized (−72 mV). Upper panel shows a fragment of intracellular activity of TC neuron. Bottom left shows superimposition of several fragments of intracellular activity aligned by the rising phase of spontaneous EPSPs. Amplitudes and latencies to peak of LTSs depended on the preceding membrane potential. Right, topographical and contour plots of EPSPs leading to an activation of LTSs. Sweeps at progressively depolarized values of the membrane potential (bottom to top); (left to right) time; colors code the voltage. Bottom plots show the gradual nature of LTS in amplitude (left) and time (right). Lines on plots represent polynomial fits.

LTSs were different during various epochs recorded from the same neuron. Thus, different TC neurons are tuned to a highly restricted frequency range of the intrinsic delta oscillation.

Spindle oscillations are also thalamically generated. Our results show that the LTSs generated during spindles are of highly variable amplitudes. Indeed, spindles recorded in TC neurons represent waxing and waning IPSPs. The highly variable amplitudes of hyperpolarizations during different epochs within a spindles sequence create conditions for the partial de-inactivation of T-channels and for the generation of partial LTSs. On the other hand, a high conductance during IPSPs in TC neurons (Ulrich and Huguenard, 1997) will have a shunting influence on the LTSs generated during the spindles. One example where an IPSP truncates the LTS is shown in Fig. 1 (right column). The spindles were induced by thalamic stimuli. The end of the current pulse was ad-

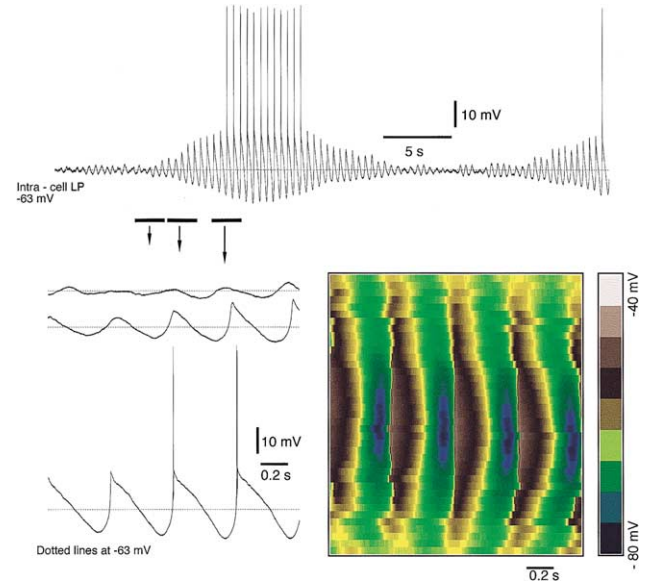


Fig. 5. Waxing and waning delta activity in LP thalamocortical neuron of decorticated cat (ketamine–xylazine anesthesia). Periods of delta-like oscillation start from subtle fluctuations of the membrane potential. The amplitude of such activity starts and declines without changes in frequency (2.2 Hz). Periods indicated by horizontal bars are expanded below. A topographical plot of delta-like activity emphasizes the stable frequency of delta-like activity regardless the amplitude of LTSs (right). Successive sweeps aligned by the maximal depolarization during LTS (bottom to top); (left to right) time; colors code the voltage.

justed to occur during the initial phase of the second IPSP in the evoked spindles. The comparison between responses to identical intracellular current pulses in the temporarily silent network (Fig. 1, left column) and responses to the same current pulses during thalamic shocks (Fig. 1, right column) shows that on all occasions the rebound LTS during spindles was significantly delayed and was mostly induced as a rebound to the second IPSP within the evoked spindle sequence. Our modeling results support the idea that the RE-evoked IPSP is an important factor in LTS termination (see Fig. 3C). Doublets of spikes in an RE cell (not shown) would be evoked by direct stimulation of this cell at different time instants during the LTS in a TC neuron. In all cases the IPSP terminated the LTS. A strong IPSP was required to terminate the LTS during its initial phase.

In barbiturate-anesthetized animals we studied the dependency of the maximal depolarization reached by TC neurons during the LTSs as a function of maximal hyperpolarization recorded during preceding IPSPs (Fig. 7). During spindles, the declining phase of IPSPs generally did not reach the baseline level, and the majority of IPSPs did not trigger an LTS. When LTSs were generated, their amplitudes were highly variable (see the plot in Fig. 7). This variability in the LTS amplitude has at least two sources. The first is the gradual nature of intrinsically generated LTSs (see above), while the second is a shunting effect of spindle-related IPSPs that truncate LTSs.

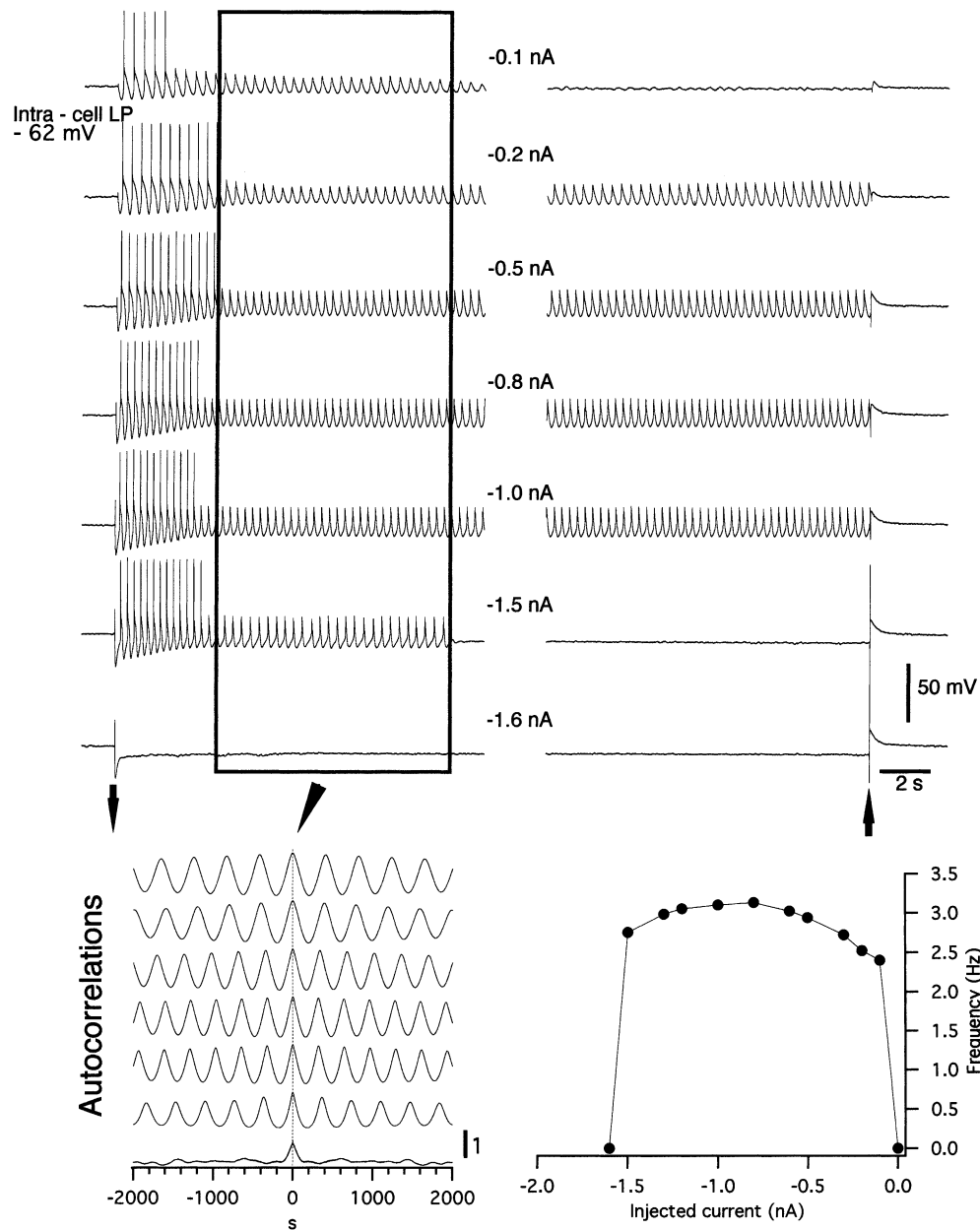


Fig. 6. The frequency of clock-like delta oscillation does not depend on the amplitude of the LTS and only slightly depends on the injected hyperpolarizing current (barbiturate anesthesia). Upper panel shows intracellular recording from LP thalamocortical neuron during periods free of spindles. Long lasting (more than 30 s) hyperpolarizing current pulses as indicated by arrows were intracellularly applied to the neuron. Fragments indicated by gray rectangle were used to calculate autocorrelations (shown below). Plot at bottom right shows the dependency of frequency of intrinsically generated delta activity from the injected current.

3.3. Spindle synchronization and spindle termination

It is thought that spindles are generated as result of an interaction between inhibitory RE neurons that fire Ca^{2+} -dependent spike-bursts, which produce IPSPs in TC neurons, and Ca^{2+} rebound excitation of TC neurons that, in turn, re-excite the RE neurons. To sustain this oscillatory activity, the network has to be perfectly synchronized. Synchronization is achieved at the beginning of spindles in TC neuronal pairs where the IPSPs are produced with delays

shorter than 1 ms (see dual intracellular recording in Fig. 10 of Timofeev and Steriade (1996)). However, approximately 30% of TC neurons do not produce rebound LTS during spindles, though they are able to generate LTSs in response to hyperpolarizing current pulses. The example in Fig. 8, shows dual intracellular recordings from a VL-TC neuron and a peri-VL-RE neuron in a decorticated animal, together with field potentials recorded from the intact contralateral cortex. Both the VL and RE neurons displayed spindle oscillations in close time relations, although the LTS rebound

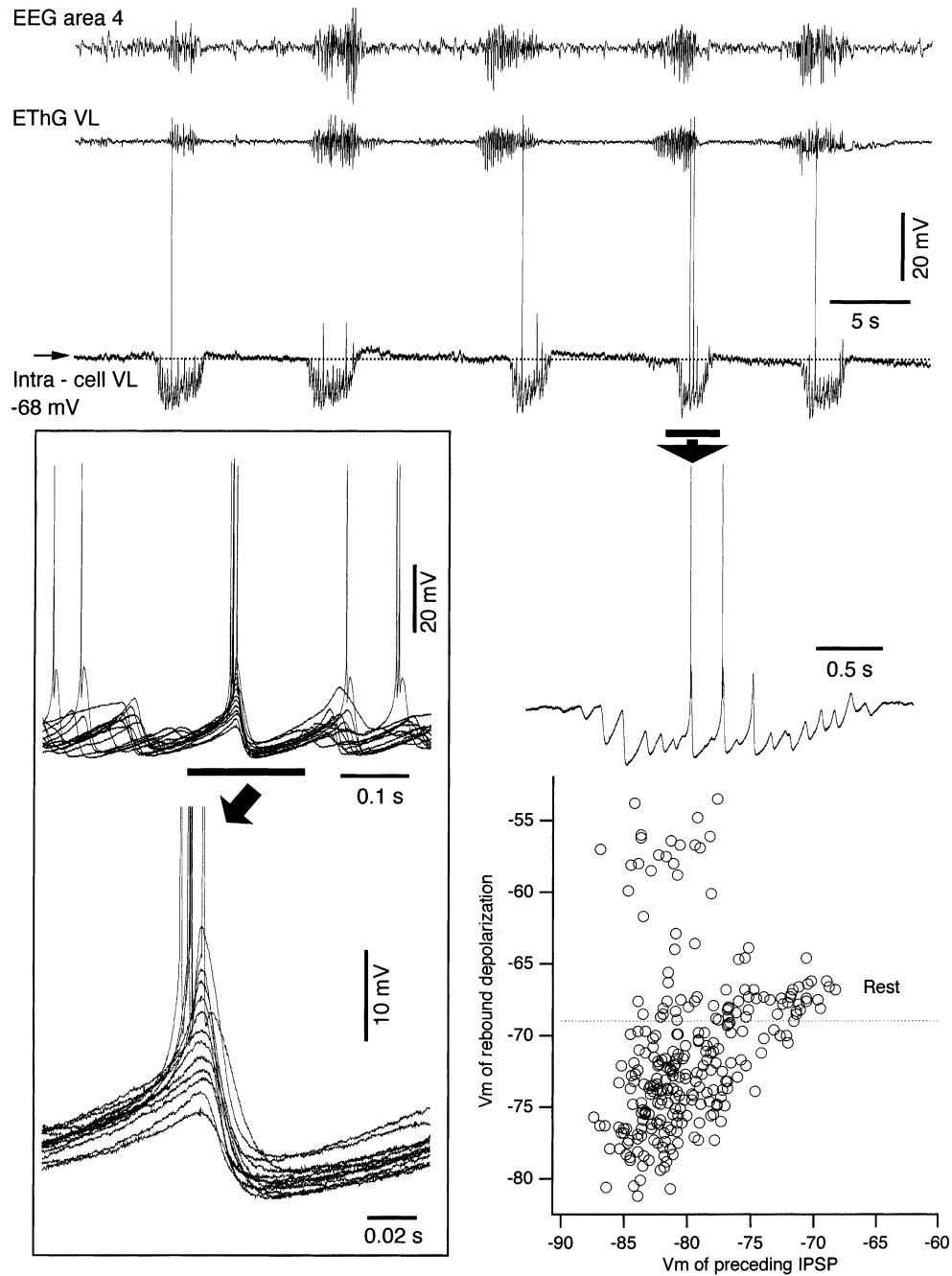


Fig. 7. LTSs are graded during spindle oscillations. Simultaneous field potential and intracellular recordings from cortical area 4, and thalamic VL nucleus (barbiturate anesthesia). One spindle marked by horizontal bar is expanded as indicated by arrow. Three LTSs of different amplitude are generated during this spindle; two of them are crowned by sodium spikes. Plot below shows the maximal depolarizing voltage reached by the neuron during IPSP repolarization phases and rebound depolarization as a function of maximal hyperpolarization during preceding IPSPs. Inset shows superposition of several sweeps aligned by the maximal depolarization during spindles.

spiking was not observed in the TC neuron and spikes were only occasionally recorded in the RE neuron. Moreover, with rare exceptions (middle sequence in Fig. 8), the spikes from the RE neuron were not generated during the onset of IPSPs in the TC neuron, as previously shown (Bal et al., 1995a,b; Timofeev and Steriade, 1996; Kim and McCormick, 1998), but at any time during the spindle. These

results suggest that the intrathalamic RE–VL network is not fully synchronized.

A detailed visual examination of spindles in TC neurons indicated that the patterns of spindle oscillations were different in the early and the late phases of a spindle sequence (Fig. 9). Superposition of intracellular activity of the same neuron in the earliest part of spindles showed that (a) full

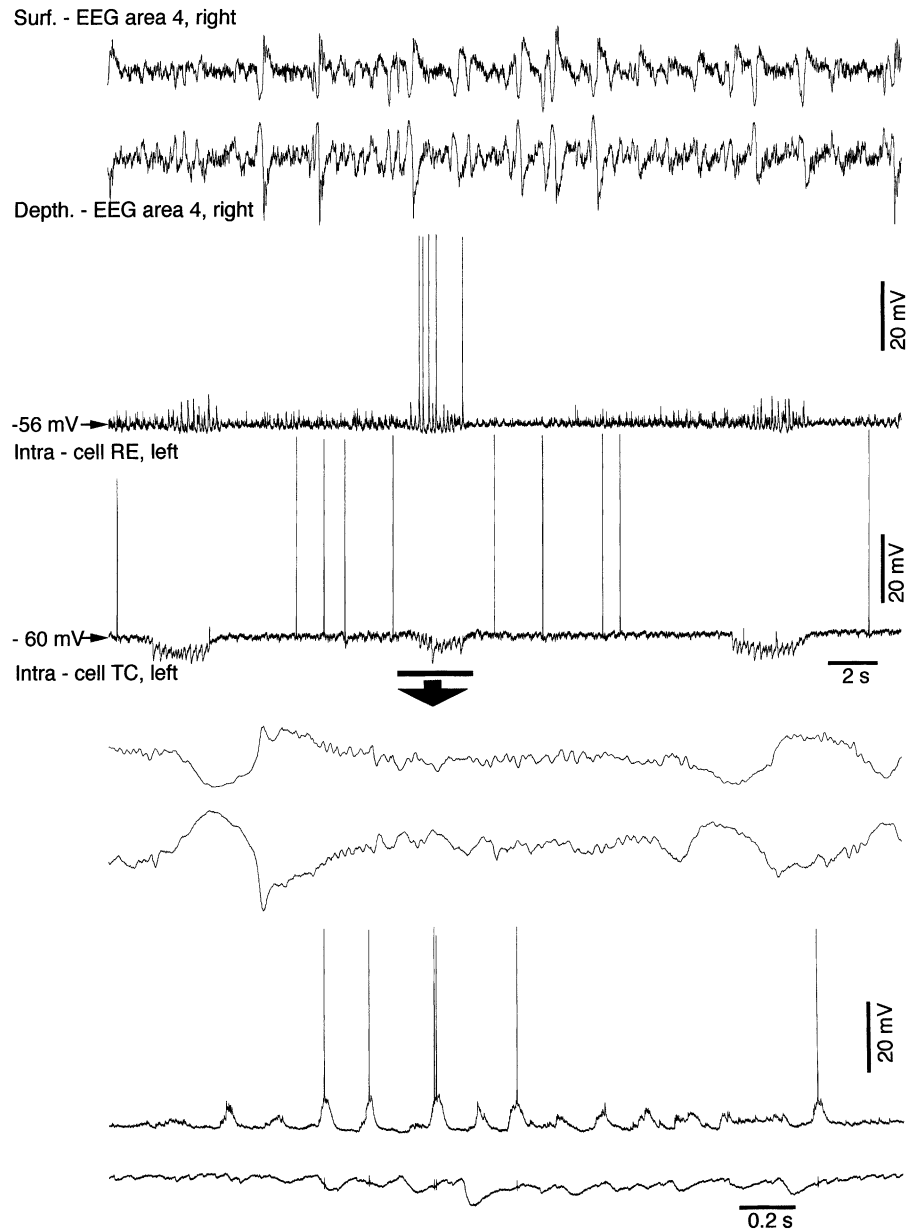


Fig. 8. Some thalamocortical neurons do not display LTSs during the spindle oscillations. Dual intracellular recording from RE and TC neurons during spindle activity in decorticated cats (ketamine–xylazine anesthesia). Two top traces are EEG recordings from right, intact hemisphere; two traces below are simultaneous intracellular recordings from RE and TC neurons. Fragment indicated by horizontal bar is expanded at bottom. In this cell pair the firing of RE neuron does not correspond to the onsets of IPSPs in TC neuron.

LTSs crowned by spike-bursts were not generated from the very onset of spindles, and (b) the activity was highly rhythmic and successive spindles were generated at similar frequencies. LTSs were generated only after several cycles of IPSPs, and, because of the intrinsic variability of their latencies (see Figs. 2 and 3), the LTSs occurred with a significant jitter. Such fluctuations in LTSs' latencies would depolarize RE neurons non-rhythmically and thus contribute to spindle termination due to asynchronous firing of RE neurons. This seemed indeed to be the case. The superposition of spindle waves by the onset of last IPSPs revealed the absence of

periodicity in successive components of the spindle sequence (Fig. 9).

To further explore the mechanisms underlying the termination of spindles, we simulated a one-dimensional network of RE and TC cells. The parameters of the RE network were set up in a way that sustained oscillations in the RE population isolated from TC input were induced. These oscillations depended on lateral inhibition between RE cells, as previously described in Destexhe et al. (1994). TC cells oscillations were maintained by RE-evoked IPSPs; however, the TC → RE feedback connections were absent

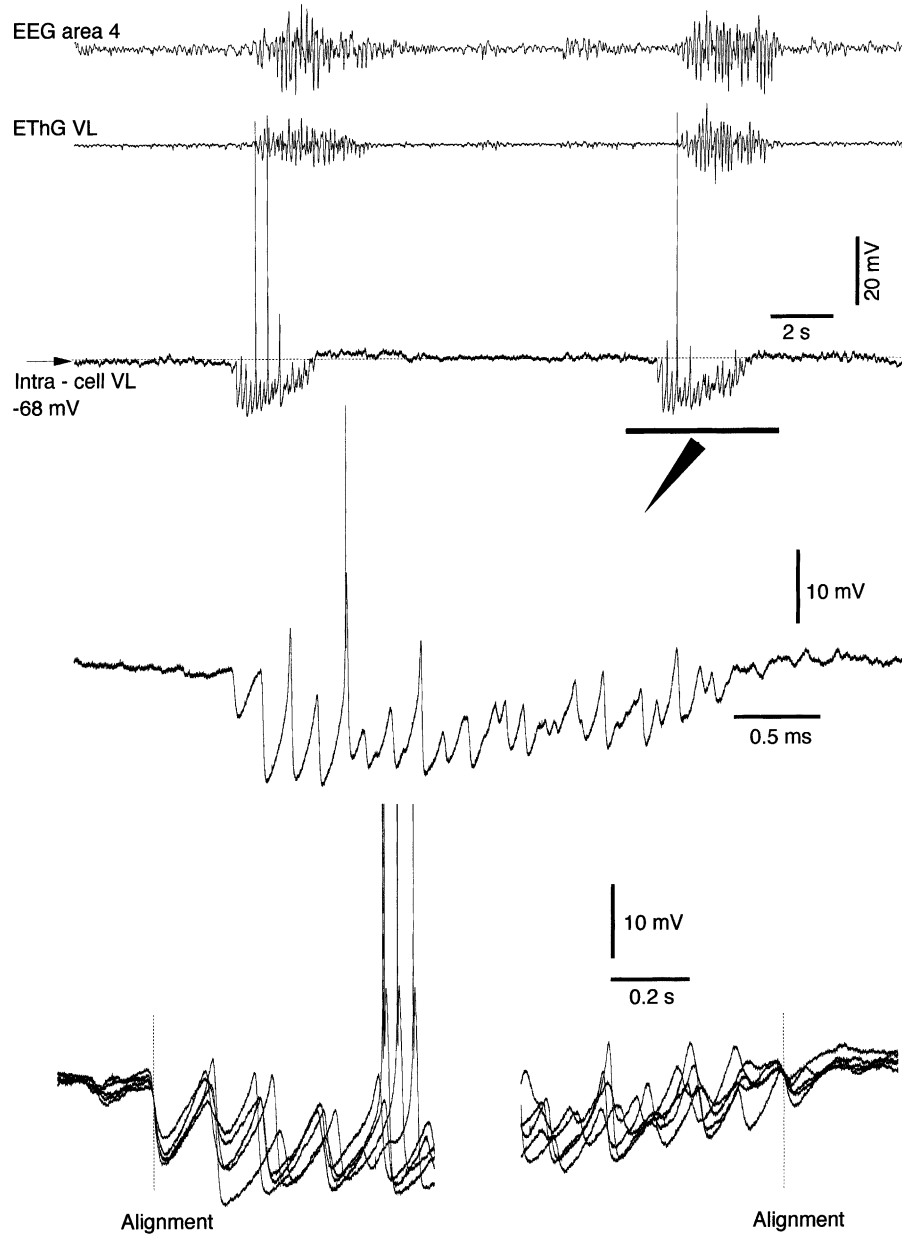


Fig. 9. Spindles are characterized by a high level of rhythmicity at their beginning and by a low level of rhythmicity at their termination. Simultaneous field potential and intracellular recordings from cortical area 4 and thalamic VL nucleus (barbiturate anesthesia). One spindle marked by horizontal bar is expanded, as indicated by arrow. At the bottom left, the beginnings of five spindle sequences are superimposed and aligned by the steepest hyperpolarizing points of first large amplitude IPSPs. At the bottom right, the endings of the same five spindle sequences are aligned by the steepest hyperpolarizing points of last IPSP.

(Fig. 10, left) and the oscillations continued infinitely. In the second network shown in Fig. 10 (right) the TC → RE AMPA-mediated connections were preserved and the RE cells oscillated at full network frequency (~ 10 Hz). After about 2 s, the oscillations were terminated not only in the TC network, but in the RE network as well. Two factors contributed: (a) Ca^{2+} up-regulation of I_h in TC cells which was, however, reduced by 50% compared with previous models (Destexhe et al., 1996; Bazhenov et al., 2000a,b),

and (b) depolarizing inactivation of the low-threshold Ca^{2+} current in RE neurons, as a result of powerful and non-synchronous barrages of TC-evoked EPSPs. The synchrony of TC input was reduced because of the strong variability of the LTS delay times (see Figs. 2–4). Note that, although TC oscillations were terminated partially as a result of I_h up-regulation, this factor did not affect activity in the RE network, which was terminated as a result of synaptic depolarizing input from TC neurons.

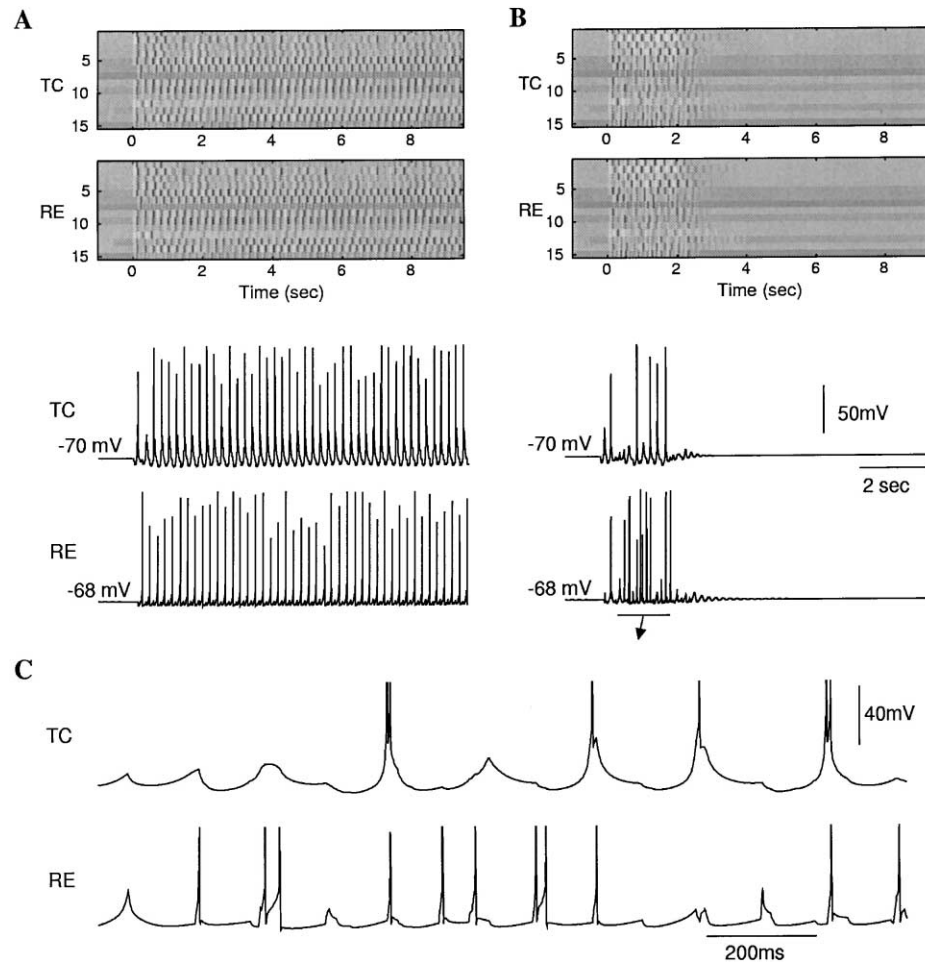


Fig. 10. Network model showing the effect of TC synchronization on spindle oscillations. (A) Without TC \rightarrow RE synaptic connections spindle-like oscillations in RE cells were maintained by RE-RE inhibition and were reflected in the TC network. (B) With intact RE-TC-RE synaptic loop and variable intrinsic parameters in TC cells, different LTS delay times occurred in different cells. Spindle oscillations were terminated after about 3 s. (C) Expanded traces of the membrane potentials from (B).

3.4. The depolarizing input of corticothalamic neurons facilitates spindle termination

We recorded intracellular activities in 578 cortical neurons from barbiturate-anesthetized cats. One hundred fifty-seven cortical neurons from area 4 were recorded simultaneously with TC neurons from the VL nucleus. These cells were classified by their intrinsic responses to depolarizing current pulses on four electrophysiological types (see Section 3.1). The majority of recorded neurons responded to thalamic stimuli applied to corresponding nuclei with EPSP-IPSP sequences or with primary IPSP, and they were implicated in spontaneous spindle activity. The spectra of activity patterns displayed by cortical neurons during spindles ranged from following every wave in simultaneously recorded TC neurons to a tonic depolarization that lasted for the whole duration of spindles. However, the majority of cortical neurons displayed a mixture of these two patterns. Generally, at the beginning of a spindle sequence the cortical neurons were

phase-locked with TC neurons, whereas from the middle to the end of spindles cortical neurons were tonically depolarized. This is illustrated in Fig. 11, which shows two recorded pairs of cortical and TC neurons, where the same TC neuron was recorded successively with one, and later with another, cortical neuron. In these both pairs, the spindle started with a series of IPSPs of TC neurons, probably reflecting the activity of RE neurons. Rebound Ca^{2+} spikes accompanied by Na^{+} spikes appeared in the TC neuron when both cortical neurons started to spindle following the spike-bursts of TC neurons (Fig. 11, see spike-triggered average, STA by TC neuron). During later phases of spindles, neocortical neurons became tonically depolarized until the end of the spindle. The cortical neuron displayed on the right in Fig. 11 had a more depolarized membrane potential and, accordingly, fired more spikes. The firing of cortical neurons during the late phase of spindles could occur at any time (see arrows in Fig. 11, right, middle). The STA by the activity of neocortical neurons did not reveal a phase relationship between

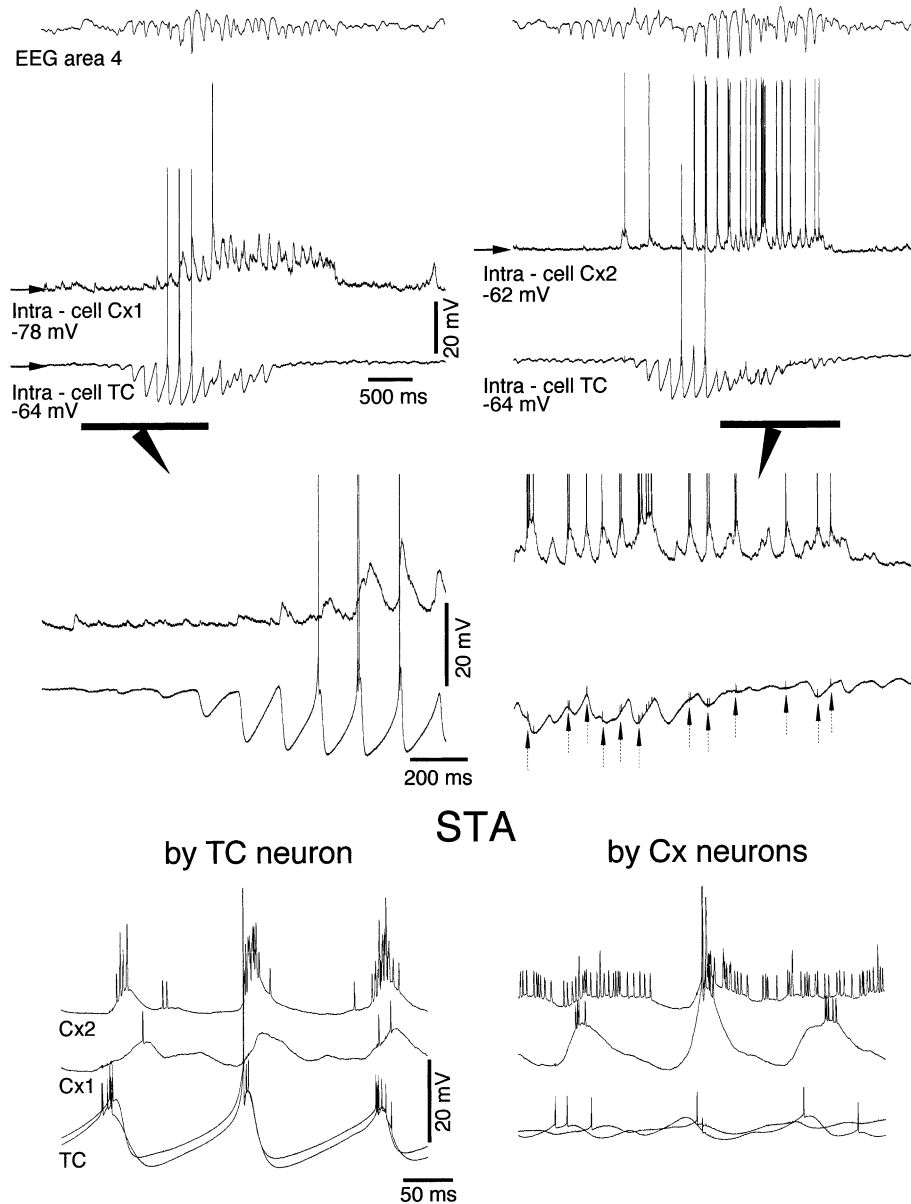


Fig. 11. Activity of cortical neurons may desynchronize thalamic spindle activity (barbiturate anesthesia). Two cortical neurons, impaled successively (left and right) were recorded simultaneously with the same thalamocortical neuron. At bottom, spike-triggered averages (STA, $n = 10$) by spikes of thalamocortical neuron shows that cortical neurons follow firing of TC neuron (left) and that IPSPs of TC neuron are not phase-locked with firing of cortical neurons (right).

the cortical and TC neurons indicating that the depolarization of cortical neurons was maintained either by intrinsic depolarizing currents of cortical neurons or by activity of intracortical network (Fig. 11).

In decorticated animals anesthetized with ketamine–xylazine the number of IPSPs in TC neurons during the waning part of spindles was 16.5 ± 5.2 (mean \pm S.D.); in intact-cortex animals anesthetized with barbiturate, we found 14.5 ± 5.3 IPSPs and in intact-cortex animals anesthetized with ketamine–xylazine, the number of IPSPs was 3.0 ± 1.1 . Given that barbiturates significantly diminish

cortical activity, these data suggest that the presence of an active cortical network (such as under ketamine–xylazine anesthesia) strongly reduced the duration of the waning part of the spindle, leading to its faster termination. This possibility was further investigated in computational models.

The model was used to test the hypothesis that the tonic activity of corticothalamic fibers could strongly depolarize RE and TC neurons, resulting in spindle termination due to inactivation of rebound Ca^{2+} spike-bursts. The model included four layers of neurons, RE–TC–PY–IN. In this model the intrinsic parameters among different TC cells

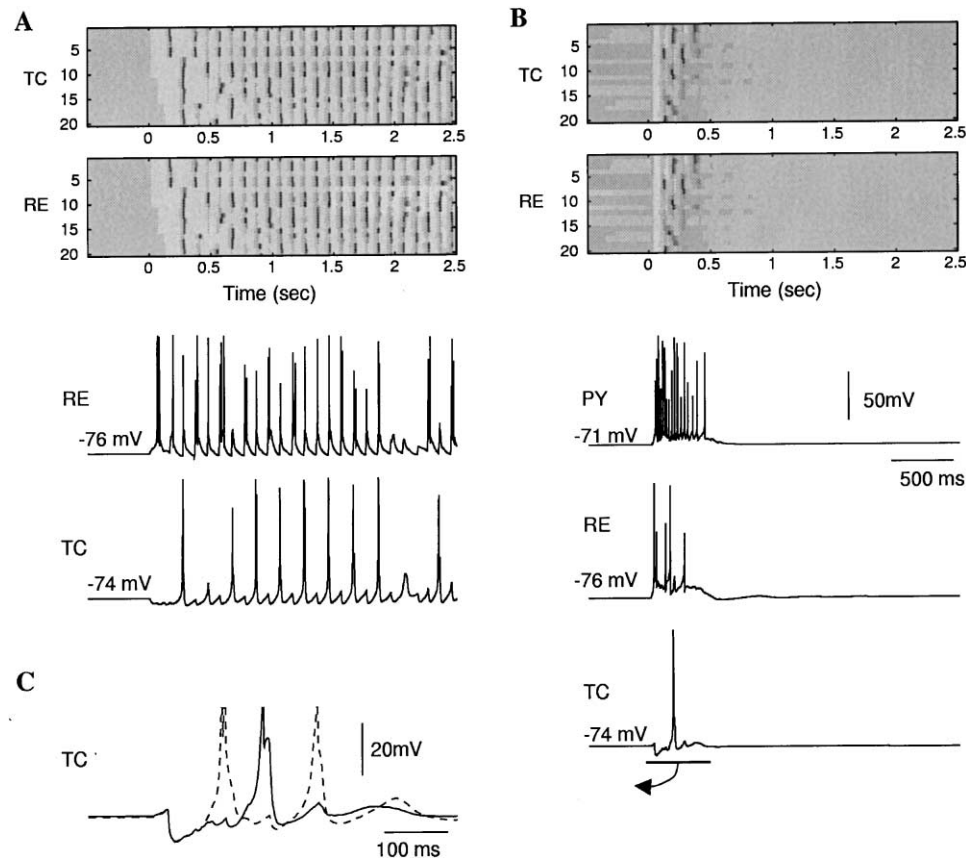


Fig. 12. Effect of corticothalamic feedback on spindle oscillations in thalamocortical network model. (A) Thalamic network disconnected from cortical input. Weak I_h up-regulation in this model was not strong enough to terminate the spindle, which continued infinitely. (B) Intact thalamocortical system. Activity patterns in IN–PY network were maintained by PY–PY excitation and persistent sodium current. Corticothalamic input depolarized RE and TC cells and terminated spindle oscillations after a few cycles. (C) Expanded traces for two neighboring TC cells (solid and dashed lines) from network shown in (B).

were identical except for variability in K^+ leak current. The RE–TC network isolated from cortical input oscillated infinitely (Fig. 12A). Up-regulation of I_h alone was not sufficiently strong to terminate spindle. When the corticothalamic feedback was included, the spindles in the RE–TC network resembled the waning spindles observed during the slow sleep oscillation in ketamine–xylazine anesthetized cats (Contreras and Steriade, 1996; Timofeev and Steriade, 1996) and terminated only after a few cycles (Fig. 12B; see also extended plot in Fig. 12C). The main factor contributing to spindle termination was a powerful and asynchronous PY \rightarrow RE input depolarizing RE cells that suppressed rebound oscillations in the RE–TC circuit. The cortical network displayed depth-negative waves of the slow oscillations, similar to those observed in naturally sleeping cats (Steriade et al., 2001; Timofeev et al., 2001; Bazhenov et al., 2000a), which promoted faster spindle termination. These patterns were maintained by lateral PY–PY excitation and I_{NaP} and were terminated after 0.5–1 s as a result of Ca^{2+} -dependent K^+ current activation and a depression of excitatory interconnections between PY cells (Bazhenov et al., 2000a; Timofeev et al., 2000).

4. Discussion

We used intracellular recordings and computational models to show that (a) the LTSs of TC neurons, generated from hyperpolarized levels that are seen in anesthetized and naturally sleeping animals are extremely variable in their amplitudes and latency to peak; these graded features of the LTS amplitude did not significantly affect the frequency of intrinsically generated thalamic delta activity; (b) EPSPs and IPSPs affected the LTS, with the IPSPs either significantly delaying the LTS generation or truncating them; (c) the variability in LTS latencies, due to their intrinsic properties and/or interaction with synaptic potentials, induced desynchronization in thalamically generated spindle activities and contributed to their termination and (d) the cortical network received spindle-related TC volleys and responded either in a phase-locked manner or produced sustained depolarization with irregular firing; this firing, which outlasted thalamic spindles in some cortical cells, depolarized both RE and TC neurons and contributed to spindle termination. The network model of thalamocortical system confirmed the interpretation of

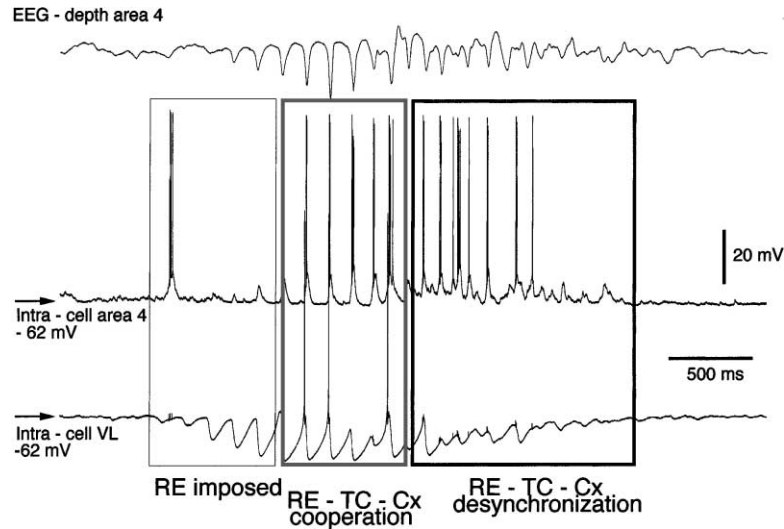


Fig. 13. Three phases of a spindle sequence. Dual intracellular recording of cortical and TC neuron. (1) Initial phase consists of series of IPSPs in TC neurons that are not followed by rebound spike-burst, suggesting that they are imposed from RE network. Spontaneous firing of some cortical neurons may trigger activities of RE network. (2) During the middle phase of the spindle, the rebound spike-bursts of TC neurons excite both RE and cortical neurons. The activity of cortical, RE and TC neurons is phase-locked. (3) At the end of spindles cortical neurons no longer fire in phase-locked manner. This firing induces depolarization of both RE and TC neurons that create conditions for the spindle termination.

these experimental results by simulating each of these mechanisms.

4.1. Mechanisms of spindle generation and termination

There are at least three phases with different underlying mechanisms that contribute to spindles (Fig. 13). The early phase of spindles (first several cycles) originated in the thalamic RE nucleus. This is based on the fact that the isolated RE nucleus is able to generate spindles (Steriade et al., 1987) and TC neurons deprived of RE connections do not show spindle activities (Steriade et al., 1985). During the early three to four IPSPs composing the spindle, TC neurons did not display rebound spike-bursts (Bazhenov et al., 2000b), suggesting that the return TC–RE connection was not contributing to the early phase of a spindle sequence. Generally, the early part of spindles was not seen or was less marked at the neocortical level. The events at the spindle onset are not fully understood. One possibility is that synchronized events in corticothalamic neurons during the slow sleep oscillation may excite both RE and TC neurons and result in the initiation of spindles in different thalamic and cortical territories (Contreras et al., 1996). Another mechanism is based on self-sustained RE activity: the relatively hyperpolarized membrane potential of RE neurons (slightly more negative than -70 mV) that occurs during slow-wave sleep can reverse IPSPs and directly trigger the LTSs of RE cells (Bazhenov et al., 1999). Even a small fraction of RE neurons hyperpolarized below the reversal potential for GABA_A IPSP is sufficient to maintain self-sustained activity and spindles in RE thalamic network (Houweling et al., 2000). Spindles may even be driven by some processes that

occur outside thalamocortical networks, like the activity in ventral pallidum that induces IPSPs in some RE neurons (Lavin and Grace, 1994), which would create conditions for the spindle generation by the RE neuronal network.

The middle phase of spindles is most likely produced in the generally accepted way (Steriade et al., 1985, 1993a; Steriade and Llinás, 1988; von Krosigk et al., 1993): RE neurons induce IPSPs in TC neurons, the end of IPSPs is associated with rebound spike-bursts that excite both RE and cortical neurons, and RE spike-bursts impose subsequent IPSPs onto TC neurons. Many cortical neurons follow TC neurons in a phase-locked manner and fire Na⁺ spikes. Corticothalamic neurons send feedback excitation to both RE and TC neurons that enhances spindles (Contreras and Steriade, 1996).

The termination of spindles may be mediated by three different mechanisms. (a) First, during the waxing phase of spindles TC neurons are hyperpolarized to a level that significantly activates I_h and repolarizes TC neurons, thus preventing their rebound spike-bursts (Bal and McCormick, 1996). (b) Second, repetitive stimulation of the dorsal thalamus with low intensity pulse-trains at spindle frequencies induces decremental responses in RE neurons (Timofeev and Steriade, 1998). This might mediate a depression of inhibition induced by rhythmic volleys from RE neurons to TC neurons (Steriade and Timofeev, 1997; von Krosigk et al., 1999). Since the primary source of spindle activity is located within RE nucleus, the relative role of I_h and depressed inhibition in TC neurons are probably not essential in the termination of spindle activity in vivo. (c) A third mechanism for the termination of spindle depends on the desynchronization of activity, based on dissimilarity of intrinsic responses in different cortical and TC neurons. There

are several sources of desynchronization that facilitate spindle termination. The first is related to the generation of LTS with different delays from the onset of IPSP. The asynchronous burst firing of TC neurons will keep the membrane potential of RE cells at relatively depolarized levels, thus preventing the de-inactivation of T-channels and diminishing the probability of burst firing. Barrages of EPSPs from prethalamic relay stations (e.g. cerebellum) may produce a small, but long-lasting, depolarization and decreased input resistance of TC neurons that could desynchronize the thalamocortical network and disrupt the spindles (Timofeev and Steriade, 1997; Bazhenov et al., 2000a,b). Because the trains of prethalamic EPSPs would occur only randomly, the most important source of spindle desynchronization, leading to the decrease in their duration, is probably long-lasting spike-trains from neocortical neurons. Several mechanisms may be involved: (a) IB neurons fire with bursts that may significantly outlast the duration of thalamically generated EPSPs (Baranyi et al., 1993). (b) Slightly depolarized FRB neurons (some are corticothalamic projecting cells) could fire high frequencies, non-accommodating trains of spikes throughout the spindle (Steriade et al., 1998). Those bursting neurons would recruit other cortical neurons into an excited state that is out-of-phase with the thalamic neurons. (c) In addition, we have recently shown that short depolarizing inputs to cortical neurons may elicit firing responses outlasting the stimulus by tens of milliseconds (Timofeev et al., 2000), producing excitation in the network with up to 180° phase shift. (d) Strong depolarizing cortical inputs onto thalamic (primarily RE thalamic) neurons will prevent the generation of LTSs and thus will lead to the spindle termination.

The present paper has explored the interaction between the intrinsic neuronal properties of neurons and spontaneous network-generated activities, with emphasis on spindle oscillations. Under different conditions the intrinsic currents in neurons can enhance network-generated activities or terminate them. Future experiments will investigate the precise phase relations of intrinsically generated potentials with synaptic responses in various forms of oscillatory behavior. If the aforementioned scenario of spindle termination holds, then stimulation of cortical areas with brief pulse-trains between spindle waves should terminate the spindles. Such stimulation might also be an effective tool to control other oscillatory events related to hypersynchronization such as paroxysmal epileptic discharges or Parkinson's disease.

Acknowledgements

We thank P. Giguère and D. Drolet for excellent technical assistance. Supported by Medical Research Council of Canada, Human Frontier Science Program, Fonds de la Recherche en Santé du Québec and Savoy Foundation, and the Howard Hughes Medical Institute.

References

- Alzheimer, C., Schwindt, P.C., Crill, W.E., 1993. Modal gating of Na⁺ channels as a mechanism of persistent Na⁺ current in pyramidal neurons from rat and cat sensorimotor cortex. *J. Neurosci.* 13, 660–673.
- Andersen, P., Andersson, S.A., 1968. Physiological basis of the alpha rhythm. In: *The Neuroscience Series*. Appleton-Century-Crofts, New York.
- Bal, T., McCormick, D.A., 1996. What stops synchronized thalamocortical oscillations? *Neuron* 17, 297–308.
- Bal, T., von Krosigk, M., McCormick, D.A., 1995a. Role of the ferret perigeniculate nucleus in the generation of synchronized oscillations in vitro. *J. Physiol.* 483, 665–685.
- Bal, T., von Krosigk, M., McCormick, D.A., 1995b. Synaptic and membrane mechanisms underlying synchronized oscillations in the ferret lateral geniculate nucleus in vitro. *J. Physiol.* 483, 641–663.
- Ball, G.J., Gloor, P., Schaul, N., 1977. The cortical electromicrophysiology of pathological delta waves in the electroencephalogram of cats. *Electroencephalogr. Clin. Neurophysiol.* 43, 346–361.
- Baranyi, A., Szenté, M.B., Woody, C.D., 1993. Electrophysiological characterization of different types of neurons recorded in vivo in the motor cortex of the cat. I. Patterns of firing activity and synaptic responses. *J. Neurophysiol.* 69, 1850–1864.
- Bazhenov, M., Timofeev, I., Steriade, M., Sejnowski, T.J., 1998a. Cellular and network models for intrathalamic augmenting responses during 10 Hz stimulation. *J. Neurophysiol.* 79, 2730–2748.
- Bazhenov, M., Timofeev, I., Steriade, M., Sejnowski, T.J., 1998b. Computational models of thalamocortical augmenting responses. *J. Neurosci.* 18, 6444–6465.
- Bazhenov, M., Timofeev, I., Steriade, M., Sejnowski, T.J., 1999. Self-sustained rhythmic activity in the thalamic reticular nucleus mediated by depolarizing GABA_A receptor potentials. *Nat. Neurosci.* 2, 168–174.
- Bazhenov, M., Timofeev, I., Steriade, M., Sejnowski, T., 2000a. Model of slow-wave sleep and its transition to activated states in thalamocortical network. *Soc. Neurosci. Abstr.* 26, 2025.
- Bazhenov, M., Timofeev, I., Steriade, M., Sejnowski, T., 2000b. Patterns of spiking-bursting activity in the thalamic reticular nucleus initiate sequences of spindle oscillations in thalamic network. *J. Neurophysiol.* 84, 1076–1087.
- Connors, B.W., Gutnick, M.J., 1990. Intrinsic firing patterns of diverse neocortical neurons. *Trends Neurosci.* 13, 99–104.
- Contreras, D., Steriade, M., 1996. Spindle oscillation in cats: the role of corticothalamic feedback in a thalamically generated rhythm. *J. Physiol.* 490, 159–179.
- Contreras, D., Destexhe, A., Sejnowski, T.J., Steriade, M., 1996. Control of spatiotemporal coherence of a thalamic oscillation by corticothalamic feedback. *Science* 274, 771–774.
- Contreras, D., Destexhe, A., Sejnowski, T.J., Steriade, M., 1997. Spatiotemporal patterns of spindle oscillations in cortex and thalamus. *J. Neurosci.* 17, 1179–1196.
- Curró Dossí, R., Nuñez, A., Steriade, M., 1992. Electrophysiology of slow (0.5–4 Hz) intrinsic oscillation of cat thalamocortical neurones in vivo. *J. Physiol.* 447, 215–234.
- Destexhe, A., Contreras, D., Sejnowski, T.J., Steriade, M., 1994. A model of spindle rhythmicity in the isolated thalamic reticular nucleus. *J. Neurophysiol.* 72, 803–818.
- Destexhe, A., Bal, T., McCormick, D.A., Sejnowski, T.J., 1996. Ionic mechanisms underlying synchronized and propagating waves in a model of ferret thalamic slices. *J. Neurophysiol.* 76, 2049–2070.
- Galarreta, M., Hestrin, S., 1998. Frequency-dependent synaptic depression and the balance of excitation and inhibition in the neocortex. *Nat. Neurosci.* 1, 587–594.
- Gray, C.M., McCormick, D.A., 1996. Chattering cells: superficial pyramidal neurons contributing to the generation of synchronous oscillations in the visual cortex. *Science* 274, 109–113.

- Hernández-Cruz, A., Pape, H.C., 1989. Identification of two calcium currents in acutely dissociated neurons from the rat lateral geniculate nucleus. *J. Neurophysiol.* 61, 1270–1283.
- Houweling, A., Bazhenov, M., Timofeev, I., Steriade, M., Sejnowski, T., 2000. A model of reticular thalamic spindle oscillations mediated by GABA_A depolarization. *Soc. Neurosci. Abstr.* 26, 2025.
- Huguenard, J.R., Prince, D.A., 1994. Intrathalamic rhythmicity studied in vitro: nominal T-current modulation causes robust antioscillatory effects. *J. Neurosci.* 14, 5485–5502.
- Jahnsen, H., Llinás, R., 1984a. Electrophysiological properties of guinea-pig thalamic neurones: an in vitro study. *J. Physiol.* 349, 205–226.
- Jahnsen, H., Llinás, R., 1984b. Ionic basis for electroresponsiveness and oscillatory properties of guinea-pig thalamic neurones in vitro. *J. Physiol.* 349, 227–247.
- Kay, A.R., Sugimori, M., Llinás, R., 1998. Kinetic and stochastic properties of a persistent sodium current in mature guinea pig cerebellar Purkinje cells. *J. Neurophysiol.* 80, 1167–1179.
- Kim, U., McCormick, D.A., 1998. The functional influence of burst and tonic firing mode on synaptic interactions in the thalamus. *J. Neurosci.* 18, 9500–9516.
- Lavin, A., Grace, A.A., 1994. Modulation of dorsal thalamic cell activity by the ventral pallidum: its role in the regulation of thalamocortical activity by the basal ganglia. *Synapse* 18, 104–127.
- Leresche, N., Lightowler, S., Soltesz, I., Jassik-Gerschenfeld, D., Crunelli, V., 1991. Low-frequency oscillatory activities intrinsic to rat and cat thalamocortical cells. *J. Physiol.* 441, 155–174.
- Lüthi, A., McCormick, D.A., 1998a. H-current: properties of a neuronal and network pacemaker. *Neuron* 21, 9–12.
- Lüthi, A., McCormick, D.A., 1998b. Periodicity of thalamic synchronized oscillations: the role of Ca²⁺-mediated upregulation of I_h. *Neuron* 20, 553–563.
- Mainen, Z.F., Sejnowski, T.J., 1996. Influence of dendritic structure on firing pattern in model neocortical neurons. *Nature* 382, 363–366.
- McCormick, D.A., Pape, H.C., 1990. Properties of a hyperpolarization-activated cation current and its role in rhythmic oscillation in thalamic relay neurons. *J. Physiol.* 431, 291–318.
- Núñez, A., Amzica, F., Steriade, M., 1993. Electrophysiology of cat association cortical cells in vitro: intrinsic properties and synaptic responses. *J. Neurophysiol.* 70, 418–430.
- Parri, H.R., Crunelli, V., 1998. Sodium current in rat and cat thalamocortical neurons: role of a non-inactivating component in tonic and burst firing. *J. Neurosci.* 18, 854–867.
- Soltesz, I., Lightowler, S., Leresche, N., Jassik-Gerschenfeld, D., Pollard, C.E., Crunelli, V., 1991. Two inward currents and the transformation of low-frequency oscillations of rat and cat thalamocortical cells. *J. Physiol.* 441, 175–197.
- Steriade, M., Llinás, R., 1988. The functional states of the thalamus and the associated neuronal interplay. *Physiol. Rev.* 68, 649–742.
- Steriade, M., Timofeev, I., 1997. Short-term plasticity during intrathalamic augmenting responses in decorticated cats. *J. Neurosci.* 17, 3778–3795.
- Steriade, M., Deschênes, M., Domich, L., Mulle, C., 1985. Abolition of spindle oscillations in thalamic neurons disconnected from nucleus reticularis thalami. *J. Neurophysiol.* 54, 1473–1497.
- Steriade, M., Domich, L., Oakson, G., Deschênes, M., 1987. The deafferented reticular thalamic nucleus generates spindle rhythmicity. *J. Neurophysiol.* 57, 260–273.
- Steriade, M., Dossi, R.C., Nunez, A., 1991. Network modulation of a slow intrinsic oscillation of cat thalamocortical neurons implicated in sleep delta waves: cortically induced synchronization and brainstem cholinergic suppression. *J. Neurosci.* 11, 3200–3217.
- Steriade, M., McCormick, D.A., Sejnowski, T.J., 1993a. Thalamocortical oscillations in the sleeping and aroused brain. *Science* 262, 679–685.
- Steriade, M., Núñez, A., Amzica, F., 1993b. Intracellular analysis of relations between the slow (<1 Hz) neocortical oscillations and other sleep rhythms of electroencephalogram. *J. Neurosci.* 13, 3266–3283.
- Steriade, M., Jones, E.G., McCormick, D.A., 1997. *Thalamus: Organization and Function*. Elsevier, Oxford.
- Steriade, M., Timofeev, I., Dürmüller, N., Grenier, F., 1998. Dynamic properties of corticothalamic neurons and local cortical interneurons generating fast rhythmic (30–40 Hz) spike-bursts. *J. Neurophysiol.* 79, 483–490.
- Steriade, M., Timofeev, I., Grenier, F., 2001. Natural waking and sleep states: a view from inside neocortical neurons. *J. Neurophysiol.*, in press.
- Tarasenko, A.N., Kostyuk, P.G., Eremin, A.V., Isaev, D.S., 1997. Two types of low-voltage-activated Ca²⁺ channels in neurones of rat laterodorsal thalamic nucleus. *J. Physiol.* 499 (1), 77–86.
- Timofeev, I., Steriade, M., 1996. Low-frequency rhythms in the thalamus of intact-cortex and decorticated cats. *J. Neurophysiol.* 76, 4152–4168.
- Timofeev, I., Steriade, M., 1997. Fast (mainly 30–100 Hz) oscillations in the cat cerebellothalamic pathway and their synchronization with cortical potentials. *J. Physiol.* 504, 153–168.
- Timofeev, I., Steriade, M., 1998. Cellular mechanisms underlying intrathalamic augmenting responses of reticular and relay neurons. *J. Neurophysiol.* 79, 2716–2729.
- Timofeev, I., Grenier, F., Steriade, M., 2001. Disfacilitation and active inhibition in the neocortex during the natural sleep-wake cycle: an intracellular study. *Proc. Natl. Acad. Sci. USA*, in press.
- Timofeev, I., Grenier, F., Bazhenov, M., Sejnowski, T.J., Steriade, M., 2000. Origin of slow cortical oscillations in deafferented cortical slabs. *Cer. Cortex* 10, 1185–1199.
- Tsodyks, M.V., Markram, H., 1997. The neural code between neocortical pyramidal neurons depends on neurotransmitter release probability. *Proc. Natl. Acad. Sci. U.S.A.* 94, 719–723.
- Ulrich, D., Huguenard, J.R., 1997. GABA_A-receptor-mediated rebound burst firing and burst shunting in thalamus. *J. Neurophysiol.* 78, 1748–1751.
- Villablanca, J., 1974. Role of the thalamus in sleep control: sleep-wakefulness studies in chronic diencephalic and athalamic cats. In: Petre-Quadens, O., Schlag, J. (Eds.), *Basic Sleep Mechanisms*, Academic Press, New York.
- von Krosigk, M., Bal, T., McCormick, D.A., 1993. Cellular mechanisms of a synchronized oscillation in the thalamus. *Science* 261, 361–364.
- von Krosigk, M., Monckton, J.E., Reiner, P.B., McCormick, D.A., 1999. Dynamic properties of corticothalamic excitatory postsynaptic potentials and thalamic reticular inhibitory postsynaptic potentials in thalamocortical neurons of the guinea-pig dorsal lateral geniculate nucleus. *Neuroscience* 91, 7–20.
- Williams, S.R., Tóth, T.I., Turner, J.P., Hughes, S.W., Crunelli, W., 1997. The ‘window’ component of the low-threshold Ca²⁺ current produces input signal amplification and bistability in cat and rat thalamocortical neurones. *J. Physiol.* 505, 689–705.